DYNAMIC CALIBRATION OF THE NOSEBOOM SENSORS OF THE FLYING HELICOPTER SIMULATOR

A. Dittmer and S. Seher-Weiss
DLR Institute of Flight Systems, Lilienthalplatz 7, 38108 Braunschweig, Germany
antje.dittmer@dlr.de, susanne.seher-weiss@dlr.de

Abstract

For modern highly or fully automated helicopters, both the airspeed and the airflow angles have to be determined as accurately as possible. Research projects dealing with enhancements of in-flight simulation, model following or automatic trajectory control - among them the current DLR ALLFlight (Assisted Low Level Flight and Landing on Unprepared Landing Site) project – need accurate knowledge of the actual helicopter state. Due to rotor downwash, helicopter airspeed measurement in the low speed range via fuselage mounted pitot tubes is inherently prone to errors. The EC-135 Flying Helicopter Simulator (FHS) of DLR is therefore equipped with noseboom mounted sensors to enable measurements relatively unperturbed by rotor downwash effects. This paper describes the calibration of the pitot system and the airflow angle measurement vanes of this noseboom. A variant of the Simultaneous Calibration of Aircraft Data System (SCADS) technique is applied which uses wind box maneuvers to reduce wind influence during the calibration process. Similar to the flight tests performed at the National Research Council (NRC), Canada, position error correction (PEC) tower flyby maneuvers are used to verify the results obtained via the SCADS wind box technique. The calculated velocity independent correction factors obtained from the SCADS technique are compared to those from classical flight path reconstruction technique.

1. INTRODUCTION

The German Aerospace Center (DLR) operates a modified EC-135 as the Flying Helicopter Simulator (FHS) research helicopter shown in FIG.1. Several research activities like the on-going ALLFlight project need highly accurate airspeed information throughout the whole flight envelope including the low speed regime. Furthermore, modeling activities using system identification call for accurately measured airflow angles.

FIG.1. FHS with noseboom

The basic air data system (ADS) of the FHS uses a pitot tube to determine dynamic and static pressure. Due to the pitot tube being mounted below the helicopter, the accuracy of the measurement decreases with decreasing air speed as the rotor downwash negatively influences the accuracy of the ADS pressure signals. Therefore, a noseboom equipped with a pitot tube and two airflow angle vanes is mounted on the FHS.

At the National Research Council (NRC), Canada, the Simultaneous Calibration of Aircraft Data System (SCADS) technique has been developed and tested that allows to simultaneously calibrate the pitot sensor and the airflow angles. This technique uses special windbox maneuvers that combine accelerations, decelerations and beta-sweeps in a box pattern thus eliminating wind influence. The SCADS method has been successfully applied for calibrating the noseboom air data systems of the NRC research airplane and helicopter [1, 2, 3] and of the DLR research airplane ATTAS [4]. As the FHS noseboom, including the pitot tube and angle of attack and sideslip angle sensors, is identical to the one of the NRC helicopter, the SCADS calibration method is used for the FHS noseboom as well.

The paper first describes the sensors used, followed by a brief description of the flight tests performed. Next the derivation of the correction parameters is presented in detail. Finally, the calibration results are compared to those obtained by classical approaches such as tower flybys and flight path reconstruction methods.

2. FHS SENSOR SYSTEMS

For the dynamic calibration of the noseboom pitot tube and angle vanes, the following high precision instrumentation is used to derive the necessary reference data:

– INS/GPS measurements

– wind measurements for tower flyby maneuvers

Although the INS/GPS data have been shown by application of flight path reconstruction to yield accurate results [5], the measured ground speed, airspeed and height above ground for the calibration flight test are further verified by comparing them to data from the following instrumentation, respectively:

– DGPS measurements for ground velocity
– air data system measurements for air speed
– radar altitude measurements

The instrumentation used in the calibration is described in more detail in the following subsections.

2.1. Noseboom System

The FHS noseboom, depicted in FIG.2, is equipped with a pitot static system measuring dynamic and static pressure and two airflow angle measurement vanes.

FIG.2. FHS noseboom with airflow and pitot sensors

The pitot tube is gimbally mounted at the front end of the noseboom. According to its sensor specification [6], the installed head orifices allow for pressure measurement errors to be essentially zero up to angles of attack or sideslip of ± 40° at velocities from 25 kt to 200 kt.

The vane used for angle of attack measurements is mounted horizontally to the left side. The other vane, which measures sideslip, is fixed vertically to the boom.

It has to be noted that the sideslip vane does not directly measure the sideslip angle. Instead, the flank angle of attack is measured. This is due to the fact that the vanes measure the angle between the longitudinal and vertical respectively lateral airspeed component. Mathematical equations relating flank angle of attack, angle of attack and sideslip angle are given in subsection 4.3.

Airspeed dependent calibration curves both for velocity and airflow angles, obtained from wind tunnel tests, are included in [6]. The manual proposes a linear calibration curve for the correction of the airspeed error. FIG.3 shows the position error, i.e. the difference between the static pressure determined from measured altitude and normal atmospheric equations and the static pressure measured at the noseboom. It can clearly be seen that the error increases quadratically with increasing airspeed which corresponds to the observations described in [3, 4].

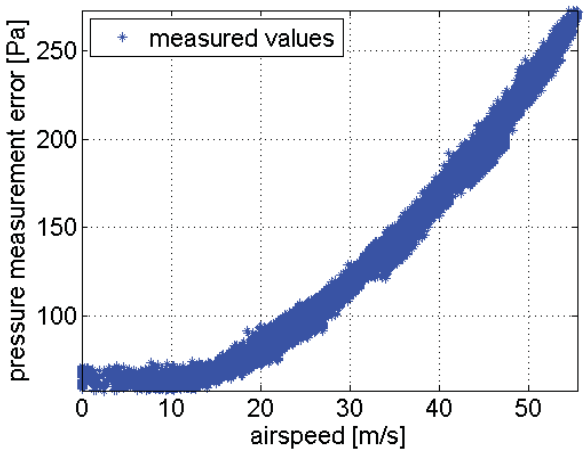

FIG.3. Pressure measurement error vs. airspeed

2.2. Honeywell INS/GPS System

The inertial navigation system (INS) Honeywell H764GU consists of INS and GPS measurements. These measurements are combined via a Kalman filter to obtain more valid information about the current geodetic position and velocities than could be gained from GPS information alone [7].

The following signals provided by this INS/GPS system are used during the calibration process as reference values for the noseboom pressure and airflow angle correction factors:

– geodetical velocity components i.e. ground speed components in north, east, and down direction
– geodetical height

In addition, angular rates and Euler angles from the INS/GPS system are used for position correction and transformation between coordinate systems.

2.3. Wind Measurement

For the flyby maneuvers, a wind measurement system of the company Thies Clima is used, that consists of an anemometer and weather vanes. The system measures the wind velocity and direction at 10 m height with a sampling interval of one second [8]. The weather vanes allow for a speed accuracy of 0.6 kt. The accuracy of the wind angle measurement should not exceed 2.5°.

The wind measured during the flight tests did not exceed 10 kt. As the runway and airport field are flat surfaces and the flybys are performed at low altitudes, it can be assumed that the wind measured on the ground is a good representation of the wind acting on the helicopter.

2.4. DGPS Data

The INS/GPS data of the Honeywell system is compared to data from a separate differential GPS system. The DGPS system used at DLR on the FHS is the system Sharpe XR6 of the company Symmetricom Ltd [9]. During all flight tests recorded, care is taken that real-time kinematic (RTK) GPS is always operational. RTK is a differential technique which uses pseudo-range as well as carrier phase measurements to compute the position of

the mobile receiver relative to the base station. This highest accuracy mode relies on having differentially corrected carrier phase measurements available to achieve position accuracies down to the low centimeter range.

The maximum difference between the two GPS systems of the data measured during all noseboom calibration flight tests performed is 3 kt in the velocity components. The INS/GPS data is thus deemed accurate enough to be used as reference data for the noseboom calibration. INS/GPS is chosen as the reference sensor instead of DGPS because in [4] the measured data are post-processed with a Kalman filter to obtain INS based GPS measurement for a flight path reconstruction (FPR). For the FHS, this Kalman filtering is already done inside the INS/GPS system.

To validate this approach, a calculation using DGPS data is performed to derive pressure and airflow correction values based on DGPS values. The derived correction coefficients and estimated wind components are compared to results obtained with INS/GPS values. The difference in estimated wind data did not exceed 0.3 kt and the difference in the coefficients is not larger than 10^{-5}. It is thus concluded that the influence of the difference between the two GPS systems can be neglected.

2.5. Air Data System

The FHS helicopter is equipped with an air data system ADS 3000 from Sextant Avionique which is part of the standard EC-135 equipment [10]. The system measures the static and dynamic pressure as well as the static air temperature. From these measurements, the indicated, calibrated and true airspeed are derived as well as the total air temperature. This is done by applying speed dependent correction factors to the measured pressures and deriving the air speed from the corrected pressures. It will be shown in section 5 that the indicated values agree well with INS/GPS measurements subtracted by the respective wind components except for very low airspeeds.

3. FLIGHT MANEUVERS

Four different flight test maneuvers are used for the FHS noseboom calibration:

– SCADS windbox
– tower flyby with constant speed
– tower flyby with acceleration/deceleration
– pace car runway flyby

The SCADS windbox maneuver and the tower flyby with constant speed have both successfully been deployed for the noseboom sensor calibration of the NRC Bell helicopter. The other two maneuvers are added to validate the correction factors for variable angles of attack and for the low airspeed range, respectively. The four maneuver types are described in more detail in the following subsections.

3.1. Windbox Maneuver

The SCADS windbox presented in [1] consists of a series of different maneuvers flown in a square pattern. The first and second sides of the box are flown with different, constant velocities. On the third and fourth side, beta-sweeps are performed while again flying with constant speed. During the whole windbox maneuver, the helicopter accelerates and decelerates only at the corner of the windbox, while airspeed at the windbox sides is kept constant. In [3], a variation of the windbox maneuver is described in which an ascent flight with maximum climb power and a descent near autorotation speed are added to the windbox described in [1]. This maneuver extension yields more variation in angle of attack compared to the basic windbox. For the FHS noseboom calibration extended windboxes as depicted in FIG.4 are flown. The maneuver definition for the six sides is as follows:

1) low constant velocity V_{lo}, accelerate by 20 kt at corner to V_{hi}
2) high constant velocity $V_{hi} = V_{lo} + 20$ kt, decelerate 5 kt at corner to V_{m1}
3) beta sweeps at constant intermediate velocity $V_{m1} = V_{lo} + 15$ kt , decelerate at corner to V_{m2}
4) beta sweeps at constant intermediate velocity $V_{m2} = V_{lo} + 10$ kt, decelerate at corner to V_{m3}
5) maximum climb power (MCP) climb at intermediate velocity $V_{m3} = V_{lo} + 5$ kt
6) autorotation descent at intermediate velocity $V_{m3} = V_{lo} + 5$ kt

The windbox pattern is planned to be repeated with the starting velocity V_{lo} varying from 20 kt to 80 kt. This approach leads to a wide range of different airspeeds in steady flight i.e. at constant speed without acceleration or deceleration at the windbox legs. The descent and climb maneuvers are used for constant angles of attack different from zero. The duration of the windbox legs is 60 s; the windbox legs' length varies accordingly from 600 m to 3000 m.

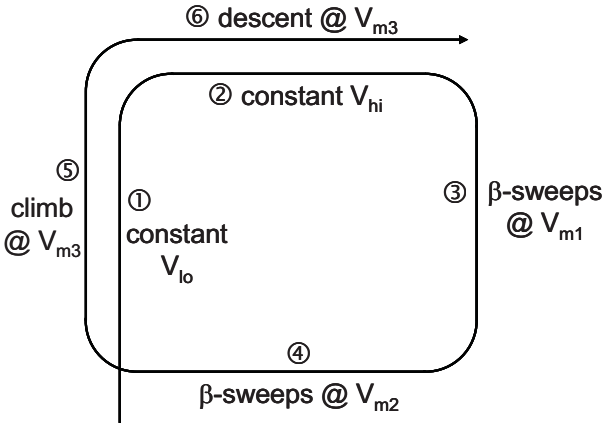

FIG.4. SCADS windbox maneuver

However, at the time of the flight tests no exact airspeed indicator for airspeeds below 30 kt was available. Hence, the airspeed of the first windbox was closer to 30 kt than 20 kt.

3.2. Tower Flyby Maneuver

To be able to obtain the position error of the static pressure measurement also by classical methods, flybys over the runway are performed. The flight test is described

in [2]:

– at a reference point with known GPS coordinates a 'baseline position' and a pressure at sea level (QNH) are recorded
– several tower flyby nap-of-the-earth flights are performed to get measurements for a calibrated point of the air data system
– several flybys over a flat surface e.g. a lake are performed for additional measurement for the calibration of the pitot sensor

The flybys are performed at an altitude of 30 ft above ground and velocities between 20 kt and 100 kt. To minimize wind influence, all flybys are flown up and down the runway. Angle of sideslip variations via beta-sweeps is integrated during some of the flybys.

As it was possible to perform several tower flybys with wind measured near the tower, no other flybys over a flat surface had to be used. This has the advantage that measured wind data is available for all PEC calibration flights.

3.3. Acceleration/Deceleration Flyby Maneuver

In order to check if the airflow correction factors are valid, some acceleration and deceleration maneuvers near the tower are included, with airspeed variation between 20 kt and 110 kt in one recorded flight test.

The SCADS windbox tests are used to calibrate the sensors for the speed range between 30 kt and 110 kt. The tower flybys with acceleration and deceleration, which increase the airspeed range slightly, show promising results regarding the validity of corrected noseboom data for low airspeed

3.4. Low Speed Pace Car Tower Flyby

To be able to determine the minimum velocity at which the noseboom sensors still yield valid airspeed measurements, some more low speed flybys are performed. During these tests, a GPS equipped car sets the reference speed by driving along the runway at constant speed while the helicopter follows at a constant distance. These pace car flybys are performed from 5 km/h (2.7 kt) to 50 km/h (27 kt).

As this flight test was performed under very calm weather conditions, the resulting airspeed is nearly constant.

4. NOSEBOOM CALIBRATION EQUATIONS

For the calibration, the true static and dynamic pressure and the true airflow angles have to be derived from INS/GPS data. Physical correlations are used to estimate the correction factors in order to minimize the difference between the true values and the corrected noseboom measurements.

The calculation of the correction factors can be broken down as follows:

– calculated static pressure based on measured INS/GPS height and QNH pressure
– air density based on calculated static pressure and measured temperature
– true airspeed derived as the difference between measured INS/GPS ground speed and measured (flybys) or estimated (windboxes) wind speed
– transformation of velocity components from geodetic to body-fixed system and to noseboom position
– calculation of dynamic pressure from GPS based air density and true airspeed;
  calculation of the pressure correction parameters
– calculation of angle of attack and sideslip from GPS and wind based air speed components;
  calculation of the airflow angle correction parameters

As the accuracy of the calculated correction parameters depends on the wind, a simplex optimization routine is used for the SCADS windboxes where no measured wind is available:

– change estimated wind parameters until the difference between the true values and the corrected noseboom values is minimal

This calculation method is shown graphically in FIG.5. The formulas used to derive the physical values are taken from [1, 2, 3, 10].

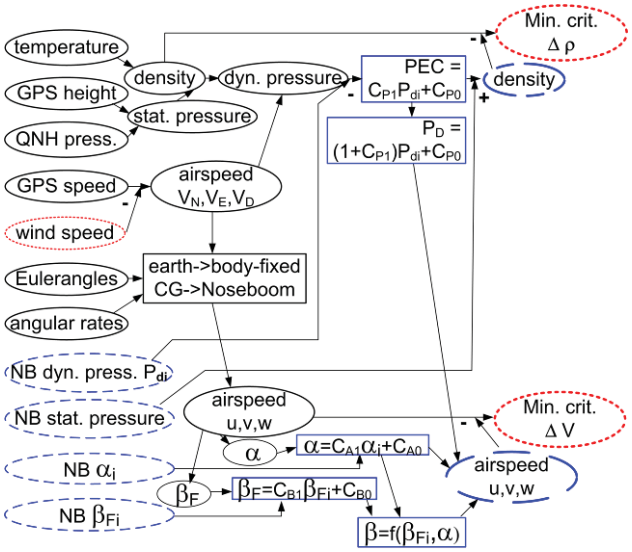

FIG.5. Flow-chart of correction coefficient calculation, estimated wind

4.1. Static and Dynamic Pressure

Generally, the static pressure measured by the pitot static system differs from the free stream pressure. This difference is primarily dependent on sensor location and vehicle airspeed. The pressure measurement error, the so called position error correction (PEC), is defined as the difference between the true dynamic pressure P_d and the indicated dynamic pressure P_{di}:

$$\text{(1)} \quad \text{PEC} = P_d - P_{di}$$

The PEC increases quadratically with increasing airspeed, see FIG.3, and is hence modeled as a first order function of dynamic pressure [3]:

$$\text{(2)} \quad \text{PEC} = C_{P0} + C_{P1} P_{di}$$

where P_{di} denotes the measured (indicated) dynamic pressure.

The true static pressure P_s can be given as the measured static pressure subtracted by the PEC [1, 2, 3, 4]:

$$(3)\quad P_s = P_{si} - \mathrm{PEC}$$

The static pressure can be derived from the INS/GPS height of the helicopter via standard atmospheric relations

$$(4)\quad P_s = P_0\left(1 + \frac{dT}{dh}\frac{h - h_0}{T_0}\right)^{\frac{n}{n-1}}$$

Here, the pressure P_0 = 101325 Pa is the standard pressure at sea level at a height of h_0 = 0 m, the temperature T_0 = 288.15 K is the standard temperature, dT/dh = -0.0065 K/m is the temperature coefficient and n = 1.234969 the polytropic exponent.

To adapt (4) to the actual atmospheric conditions, the pressure at sea level, the so called QNH pressure P_{QNH} which is provided by the tower is used in the above equation. Similarly, T_0 is to be replaced by the air temperature T_{QNH} at sea level corresponding to the current temperature as provided by the air data system. The physical dependency of density and pressure of ideal gases is modeled by [11]:

$$(5)\quad \left(\frac{\rho_1}{\rho_0}\right) = \left(\frac{P_1}{P_0}\right)^{\frac{1}{n}}$$

The air density ρ as a function of calculated static pressure and measured temperature T is defined as:

$$(6)\quad \rho = \frac{P_s}{RT}$$

where R = 287.05287 J/kgK is the gas constant. Substituting the density in (5) by (6) results in:

$$(7)\quad T_{QNH} = T_0\left(\frac{P_{QNH}}{P_0}\right)^{\frac{n-1}{n}}$$

With these two modifications, the reference value for the static pressure is derived from the INS/GPS altitude via

$$(8)\quad P_s = P_{QNH}\left(1 + \frac{dT}{dh}\frac{h - h_0}{T_0\left(\left(P_{QNH}/P_0\right)^{\frac{n-1}{n}}\right)}\right)^{\frac{n}{n-1}}.$$

The dynamic pressure derived from a pitot static system is the difference between the measured total and static pressure. Inaccuracies in the measured dynamic pressure thus directly affect the static pressure and the true dynamic pressure can be described as the sum of the measured dynamic pressure and the position error correction. Alternatively, dynamic pressure can be written as a function of speed and air density:

$$(9)\quad P_d = P_{di} + \mathrm{PEC} = 0.5\rho V_{TAS}^2$$

Using the air density, calculated from INS/GPS data and the true airspeed, derived from INS/GPS and wind data, the reference dynamic pressure P_d can be derived as described in (9).

4.2. Airflow Angles

Several noseboom characteristics which have to be considered in the airflow angle measurement are:

1) noseboom misalignment
2) noseboom deflection due to flexibility
3) transformation of the measured flank angle of attack into sideslip angle
4) rotor downwash effects
5) transformation of angles measured via INS/GPS at the center of gravity to noseboom position

The influence of these factors is evaluated and commented in [1]:

1) A static calibration leads to a misalignment tolerance of 0.3° of the noseboom [3 ,6]. Misalignment errors of this small size can be modelled as linear bias. The correction factor calculated here mainly corrects the effect of rotor downwash, but implicitly corrects the misalignment as well.

2) The system dynamic of the flown maneuvers does not excite the noseboom eigen dynamic, i.e. the elastic distortion can be neglected. To make sure that no dynamics influence the results only data measured during steady state flight is considered in the first two of the three approaches presented in section 5.

3) The sideslip angle has to be calculated from the flank angle of attack and the angle of attack. Angle of attack α and flank angle of attack β_F are defined as:

(10) $\alpha = \tan^{-1}(w/u)$,
(11) $\beta_F = \tan^{-1}(v/u)$.

The sideslip angle β is defined as

(12) $\beta = \tan^{-1}(v/U)$

and can be calculated from α and β_F via

(13) $\beta = \tan^{-1}(\tan(\beta_F)\cos(\alpha))$.

The velocity components u, v, and w are defined as helicopter airspeed components in the aircraft coordinate system in x-, y-, and z-direction, respectively. The definition of the horizontal helicopter velocity U is:

$$(14)\quad U = \sqrt{u^2 + v^2}$$

The true angle of attack and flank angle of attack are hence calculated from measured INS/GPS airspeed components.

4) To model the influence of the downwash, linear correction factors are introduced. The true angle of attack and the true flank angle of attack can be described as:

(15) $\alpha = C_{A0} + C_{A1}\alpha_i$.
(16) $\beta_F = C_{B0} + C_{B1}\beta_{Fi}$.

where α_i and β_{Fi} are the noseboom indicated values of angle of attack resp. flank angle of attack. From these corrected angles, the true sideslip is calculated, as described in (13).

5) For the calculation of the correction factors for the noseboom measured airflow angles the true airflow angles at the noseboom location have to be known. They can be derived from the true airspeed components of the helicopter. These components are derived from the

INS/GPS velocities and the estimated or measured wind speed. The speed of a vehicle is often given with reference to its center of gravity. As the exact position of the helicopter center of gravity varies with loading condition, a so-called Guidance Control Point (GCP) is defined, which is independent of the current loading state. The measured INS/GPS speed components are always given with respect to this point.

To calculate the airflow correction factors, the INS/GPS speed components are transformed to the corresponding speed components at the noseboom sensors. This linear transformation is given in [3]. It is a sum of the airspeeds acting at GCP and a vector product of the three angular rates p, q, and r and the distance between the GCP and the noseboom center in the x-, y- and z-direction of the aircraft coordinate system:

(17) $u_{GPS@NB} = u - r \Delta y_{GCP,NB} + q \Delta z_{GCP,NB}$,
(18) $v_{GPS@NB} = v + r \Delta x_{GCP,NB} - p \Delta z_{GCP,NB}$,
(19) $w_{GPS@NB} = w - q \Delta x_{GCP,NB} + p \Delta y_{GCP,NB}$,

4.3. Airspeed and ground speed

The airspeed is calculated as the difference of the INS/GPS speed and the wind speed. From the ground speed components V_{GN}, V_{GE}, and V_{GD} in the north-east-down earth coordinate system, the wind speeds are subtracted to obtain the helicopter airspeed components in the earth coordinate system:

(20) $v_x = V_{GN} - V_{WN,}$
(21) $v_y = V_{GE} - V_{WE,}$
(22) $v_z = V_{GD} - V_{WD.}$

The three components of the airspeed are transformed via the Euler matrix into the three airspeed components u, v and w of the aircraft coordinate system. The wind is estimated during the SCADS maneuvers, as no measured data is available for these flight tests which have to be performed at a certain height due to the descent near autorotation.

The wind is optimized to minimize the cost function presented in [1], a weighted sum of airspeed error and air density error. The weighting factors for this sum are unknown. The cost function chosen for the current investigation is a weighted sum of the airspeed error in m/s and the air density error in kg/m^3:

(23) $$J = \sum_{t=t_0}^{t_{end}} (x_1 \mid \Delta V \mid + x_2 \mid \Delta\rho \mid)$$

with t_0 and t_{end} as the start respectively, end time of the recorded flight test dataand the weighting factors x_1 = 1 s/m and x_2 = 1 m^3/kg.

5. CORRECTION COEFFICIENTS

The pressure correction factors C_{P0} and C_{P1}, appearing in (2), and the ones for the airflow angles, C_{A0}, C_{A1}, C_{B0} and C_B, from (15) and (16), are derived via the helicopter airspeed. The validity of the correction values depends on a good estimation of the wind acting on the helicopter.

Different methods to derive the estimated wind and the resulting correction coefficients are presented. No measured wind is available for the SCADS windbox flight tests; hence the wind must be estimated for these maneuvers. For all tower flybys, wind measurements from an anemometer near the airport tower are available. As the tower flybys are flown under calm weather condition at an altitude of only 15 m over the runway surface, the measured wind should be a good estimate of the actual wind acting on the helicopter. However, for comparison purposes, the flyby maneuvers were also evaluated with estimated wind. The correction coefficients calculated with estimated wind are then compared to the ones derived with measured wind.

5.1. Coefficients Derived with Estimated Wind

Three different calculations of the correction factors are carried out. The first and second method, called SCADS1 and SCADS2, use the windbox maneuvers to determine the correction coefficients. The SCADS1 method is the approach used in [1, 2, 3]. It calculates the correction coefficient for each windbox separately and mean values are then determined for the obtained coefficients.

For SCADS2 several windboxes are concatenated for the calculation of one set of pressure correction coefficients. The airflow correction factors are calculated using the windbox sides with the strongest variation in the respective airflow angle. For angle of attack, these are the climbs and descents on the fifth and the sixth windbox legs, see FIG.4, whereas for the flank angle the beta-sweeps, the third and forth windbox sides, are used.

The third method, system identification, uses data from the tower flybys and the pace car flights for calibration of the static and dynamic pressure. The airflow angles are calibrated with the same windbox maneuvers data used in the SCADS2 approach.

For all three methods, the estimated wind is assumed to be constant during one maneuver.

5.1.1. SCADS Windbox Coefficients

The SCADS windbox maneuvers are flown at eight different airspeed variations see subsection 3.1. Four of these maneuvers are flown twice to obtain redundant data. This leads to a total of 12 windboxes, resulting in 12 sets of correction factors for the SCADS1 approach. The mean, minimum and maximum of these values are displayed in TAB 1. Analyzing the results, it is found that the deviations of the pressure correction coefficients are unacceptably large, with a standard deviation for C_{P0} of 51.46, corresponding to a relative standard variation of 85.18%. The standard deviation of C_{p1} is 0.06 respectively 42.64%.

	C_{P0} [Pa]	C_{P1} [-]	C_{A0} [rad]	C_{A1} [-]	C_{B0} [rad]	C_B [-]
Mean	60.20	.1407	-.0014	.7596	-.0182	.7610
Max.	157.72	.2396	.0237	.8224	-.0051	.8129
Min.	-24.92	.0410	-.0201	.6278	-.0367	.6867
Std. dev.	51.46	.0601	.0140	.0605	.0104	.0421

TAB 1. SCADS1 results (separate windboxes)

The estimated SCADS1 pressure coefficients are depicted in FIG.6. Apparently, the derived values are linearly dependent, as the bias C_{P0} increases with decreasing

scale factor C_{P1}. The mean values C_{P0} and C_{P1} of the SCADS1 results are also shown in the plot. The pair of the mean values of the SCADS1 results lies on a first order regression line determined for the SCADS1 results.

The results obtained with SCADS2, explained below, and the system identification methods, explained in detail in subsection 5.1.2, lie close to this line

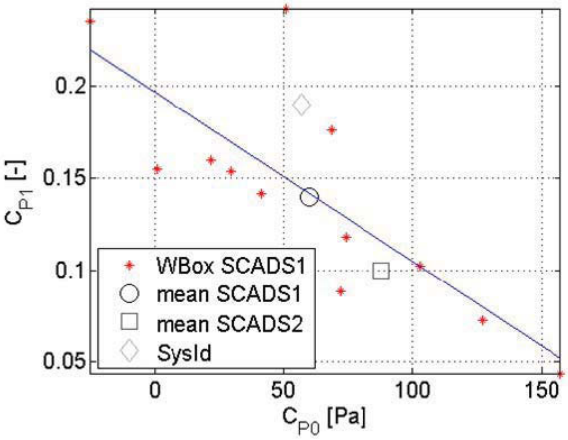

FIG.6. Pressure coefficients C_{P1} vs. $C_{P0,}$ SCADS windboxes

If the SCADS1 method is rerun with the value for C_{P1} fixed to its mean value of 0.14, the mean, maximum and minimum value for the remaining bias parameter C_{P0} are 59.41 Pa, 99.56 Pa and 24.39 Pa respectively. The mean C_{P0} = 59.4 Pa is almost identical to the one calculated with varying scale factors, C_{P0} = 60.20 Pa, with a difference between the two values of 0.13%. The absolute standard deviation between the bias factors calculated for each run is reduced to 23.25 (39%). Although the standard deviation is thereby reduced by the factor two, it is investigated if this deviation can be further reduced

It is suspected, that the linear dependency between C_{P0} and C_{P1} for the SCADS1 approach was caused by too little airspeed variation within one windbox. Therefore it is tested if a method taking into account a wider range of velocities i.e. more information, than can be provided by one windbox maneuver, can narrow the variance in both coefficients further.

If the noseboom measurement represented the real airflow angles, the correction scale factors would be equal to $C_{A1} = C_{B1} = 1$. The scale correction values $C_{A1} = C_{B1} = .76$ calculated with the SCADS1 method are considerably smaller. This might be due to the analyzed windbox data. As only two of the six windbox sides include variation of one of the airflow angles, dynamic as well as steady state data are used to obtain the correction factors. All disturbances such as wind gusts cannot be modeled and thus negatively influence the match in the airflow angles, as only constant horizontal wind is estimated for each maneuver. To minimize this effect, only the maneuvers with the largest variation in the respective airflow angle are used for calibration. Thus, to determine C_{A0} and C_{A1} from (15), all climbs and descents are concatenated and evaluated together, the correction factors determined by minimizing (23). Similarly, C_{B0} and C_{B1} from (16) are estimated from a concatenation of all beta-sweeps with (23) as cost function.

Hence, the aim of the next step is to narrow the range of the pressure correction and the airflow correction factors. This leads to the SCADS2 method: The pressure correction factors for a concatenation of four windboxes of the 12 windboxes are calculated. The first and the third set include windboxes with starting velocities V_{lo} of 20 kt, 40 kt, 60 kt and 80 kt. The second set concatenates windboxes with starting velocities V_{lo} of 30 kt, 50 kt, 70 kt and 90 kt. The angle of attack correction factors are calculated by using only the climb and descent sides of these three sets of windboxes, whereas the sideslip correction factors are derived using the beta-sweeps. Mean, minimum and maximum correction parameters are calculated using the three obtained correction factor sets. The results denoted SCADS2 and listed in TAB 2 are therefore a combination of three optimizations.

	C_{P0} [Pa]	C_{P1} [-]	C_{A0} [rad]	C_{A1} [-]	C_{B0} [rad]	C_B [-]
Mean	88.69	.1022	-.0051	. 7972	-.0283	.7974
Max.	93.79	.1091	-.0011	.8235	-.0108	.8129
Min.	86.00	.0913	-.0137	.7709	-.0674	.7820
Std. dev.	4.42	.0095	.0064	.0324	.0140	.0217

TAB 2. SCADS2 results (concatenated windboxes)

It can be seen that the SCADS2 calculations leads to considerably smaller deviations of the pressure correction factors. The correction factors C_{P0} and C_{P1} differ from the ones found by the SCADS1 method by 30%, though. The consistency of the results is to be tested. Therefore, the four values of C_{P0} of the four windboxes of one windbox set are calculated with the C_{P1} fixed to the value obtained with SCADS2 method for this set. The three mean values of the respective four bias values are derived. The results are shown in TAB 3.The largest variation in C_{P0} occurs for the third set: a relative difference of 3.8% is derived, which is considered acceptable.

Windbox sets	Concatenation/ SCADS2		Mean/ SCADS1
	C_{P0} [Pa]	C_{P1} [-]	C_{P0} [Pa]
1) 20 kt, 40 kt, 60 kt, 80 kt	86.00	.1091	85.92
2) 30 kt, 50 kt, 70 kt, 90 kt	86.28	.1061	87.17
3) 20 kt, 40 kt, 60 kt, 80 kt	93.79	.0913	97.37

TAB 3. Comparison of SCADS2 and SCADS1, SCADS1 C_{P0} values calculated with fixed C_{P1}

To be able to judge the differences in the determined pressure correction factors, their influence on the resulting velocity is to be investigated. The constant bias C_{P0} can be identified best by using low velocities resulting in pressure measurement around 0 Pa, whereas the influence of the scale correction factor C_{P1} becomes more pronounced at higher speeds. This can be deduced from the equation relating the correction coefficients, the measured and the true dynamic pressure:

$$(24)\quad P_d = C_{P0} + (1 + C_{P1})P_{di}$$

The dynamic pressure measured at DLR during the SCADS windbox flight tests varies from 50 Pa to 1500 Pa. The velocity can be calculated as:

$$(25)\ V = \sqrt{\frac{2P_d}{\rho}} = \sqrt{\frac{2[(1+C_{P1})P_{di} + C_{P0}]}{\rho}}$$

Therefore, with the air density set to ρ = 1.225 kg/m^3 the difference in velocities based on the measured pressure of P_{di} = 50 Pa and the mean pressure correction values from TAB 1 and TAB 2 is calculated as:

$$(26)\ \Delta V_{50} = V_{50,\,SCADS1} - V_{50,\,SCADS2} = 26.87\text{ kt} - 29.76\text{ kt} = -2.88\text{ kt}$$

The resulting difference is an acceptable value for low airspeeds which are inherently difficult to measure [10]. With increasing airspeed, the speed difference decreases further:

$$(27)\ \Delta V_{1500} = V_{1500,SCADS1} - V_{1500,SCADS2} = 104.29\text{ kt} - 103.46\text{ kt} = -0.83\text{ kt}$$

Next, the resulting difference in airflow angles when comparing the results from SCADS1 and SCADS2 is analyzed. For an angle of attack of 40°, the difference between SCADS1 and SCADS2 results yields a difference in angle of attack of 1.29°. It has to be noted, that the angles occurring for maximum climb power and descent near autorotation did not exceed 15°, which corresponds to a difference of values corrected with SCADS1 and SCADS2 of 0.35°. Similarly, the difference resulting at a sideslip angle of 40° is 0.877°. The maximum of all sideslip angles measured during the beta-sweep maneuvers is 20°, corresponding to a difference of 0.149°. The small difference in calculated angles suggests that the influence of the additional windbox legs data considered in the SCADS1 approach does not unduly influence the correction factors.

As velocities lower than 30 kt are not considered in the SCADS1 or SCADS2 approach, no information is available regarding which offset leads to a better fit for airspeeds between 16 kt and 30 kt. Therefore, a stepwise identification of the correction factors using the tower flybys i.e. flights varying between 16 kt and 110 kt is used for this purpose.

5.1.2. System Identification Coefficients

In addition to the SCADS method, a more conventional calibration via system identification is performed. The identification model has the INS/GPS data as inputs as well as the total air temperature, QNH pressure and the measured noseboom data. Similar to the SCADS calculation, the system identification calibration is carried out according to the flow-chart of FIG.5.

Contrary to the SCADS approaches, the correction coefficients are derived consecutively. The pressure correction factors are calculated first. The maneuvers used for this calculation are the tower flybys. With the obtained coefficients C_{P0} and C_{P1} fixed, the airflow correction coefficients are then calculated in a second, independent step using windbox data.

As the goal of the PEC calibration is to achieve the highest airspeed accuracy possible, only airspeed errors are considered for the determination of the PEC parameters. The cost function is therefore changed from (23) to:

$$(28)\ J = \sum_{t=t_0}^{t_{end}} (\Delta V)^2$$

The optimization of the unknown calibration coefficients and the wind parameters is performed using a maximum likelihood output error method [12].

For this purpose, the corrected airspeed V is derived from the corrected noseboom dynamic pressure via (25).

To cover the whole airspeed range of the FHS, all PEC flybys and all pace car flybys are evaluated together. The resulting calibration coefficients are listed in TAB 4.

C_{P0} [Pa]	C_{P1} [-]	C_{A0} [rad]	C_{A1} [-]	C_{B0} [rad]	C_{B1} [-]
58.90	.1933	-.0081	.7871	-.0125	.7909

TAB 4. System identification results

The resulting airspeed difference when comparing the SCADS2 and system identification results are 2.8 kt for a measured pressure of 50 Pa and 3.2 kt for a pressure of 1500 Pa. The corresponding differences to the mean SCADS1 values are 0.16 kt at 50 Pa and 2.36 kt at 1500 Pa.

The mean and standard deviation of the remaining differences between the INS/GPS based reference values and the values from the corrected noseboom data for all maneuvers using the results shown in TAB 4 is for all windbox and tower flyby maneuver smaller than 2 kt. Although neither the error in static pressure nor the altitude error is weighted during the identification, the resulting errors in altitude are below 8 m for the SCADS windboxes. The differences to all tower flyby reference radar heights are below 5 m, with half of the runs having a mean difference of less than 1.5°m to the reference data. The airflow angles are calibrated using the windbox maneuvers. For this second calibration step, the calibration coefficients for the position error are fixed at the values determined from the flyby maneuvers.

The windbox legs with the largest variation in the respective airflow angle are used for calibration i.e. the same data which is used for the SCADS2 method. Thus, a concatenation of all climbs and descents is chosen to determine C_{A0} and C_{A1}. Contrary to the SCADS2 method, only the error in angle of attack is weighted. The flank angle of attack correction values C_{B0} and C_{B1} from (16) are obtained from all beta-sweeps minimizing only the error in flank angle. The resulting calibration coefficients can be found in TAB 4.

Both angle measurements C_{B0} and C_{A0} from TAB 4 exhibit an offset of less than 1° and both have a relatively similar calibration factor. The difference between a measured angle of attack of 40° corrected with system identification values and an angle corrected with SCADS2 values is 0.57°. At an angle of 15°, the difference is 0.32°. The difference for a measured sideslip angle of 40° is 0.64°, and if the measured sideslip is 15°, the difference is 0.77°. The mean value and standard deviation of the remaining difference between reference values and corrected noseboom data for the two airflow angles is below 1° for all runs faster then 20 kt. For sideslip angles the mean value of the difference is below 1° for the whole airspeed range. It has to be noted, however, that the errors are each

determined by simulation over the whole maneuver including all corners and with constant wind for each maneuver. Larger errors only remain for the angle of attack at low airspeeds. These errors could probably be reduced by applying a speed dependent calibration factor in (15). This is, however, not yet deemed necessary.

As the system identification correction factors of the angles are determined from the windbox sides with the maximum angle variation, the difference to the results from the SCADS2 optimization is comparably small. For an angle of attack of 40°, the difference between the system identification and SCADS2 results, is 1.11° and for 15° the difference is 0.41°. Similarly, the difference for a sideslip angle of 40° is 1.19° and for 20° the difference is 0.59°. A comparison between mean deviations of reference data and corrected data for four SCADS windboxes and the three faster pace car runs is shown in TAB 5.

Windboxes	80 kt to 100 kt ΔV [kt]	60 kt to 80 kt ΔV [kt]	40 kt to 60 kt ΔV [kt]	30 kt to 40 kt ΔV [kt]
SCADS1	1.84	2.04	3.01	1.96
SCADS2	1.86	2.02	2.37	2.1
SysId	1.47	0.56	1.82	0.49
Pace Car Flybys	30 km/h ΔV [kt]	40 km/h ΔV [kt]	50 km/h ΔV [kt]	
SCADS1	1.16	1.75	1.94	
SCADS2	4.27	4.27	2.52	
SysId	1.42	2.37	1.88	

TAB 5. Mean deviations to reference speed

All three sets of calibration results (SCADS1, SCADS2, SysId) show good fits for the windboxes flown between 30 kt and 110 kt. The difference is smallest between the reference data and the system identification correction set. Although the values of the SCADS1 set show slightly smaller differences than the system identification values when applied at low airspeed, i.e.16.2 kt to 30 kt, the set derived via system identification is finally chosen due to overall best fit for the noseboom correction.

FIG.7 and FIG.8 show flight data corrected with system identification correction factors applied to noseboom measurements for a windbox maneuver between 80 kt and 90 kt. The corrected noseboom values are compared to the GPS based reference values and the measurements from the air data system. Changes in dynamic and static pressure, and therefore in airspeed and height, are contained in this maneuvers as well as airflow angle variations.

The variation in airspeed is largest in the first third of the data which corresponds to the first two windbox legs (see FIG.4) flown at V_{lo} = 80 kt and V_{hi} = 100 kt. The beta-sweeps are flown at the second and third leg, followed by the maximum climb power climb and the descent near autorotation which lead to angles of attack of -7° and 8° respectively. The resulting differences between GPS based reference data, corrected noseboom values, and values from the basic air data system are displayed in FIG.8. The peaks in the dynamic pressure difference are due to wind gusts which are not included in the estimated wind model. The absolute difference to the ADS airspeed is below 4 kt. The difference in airflow angle is largest at

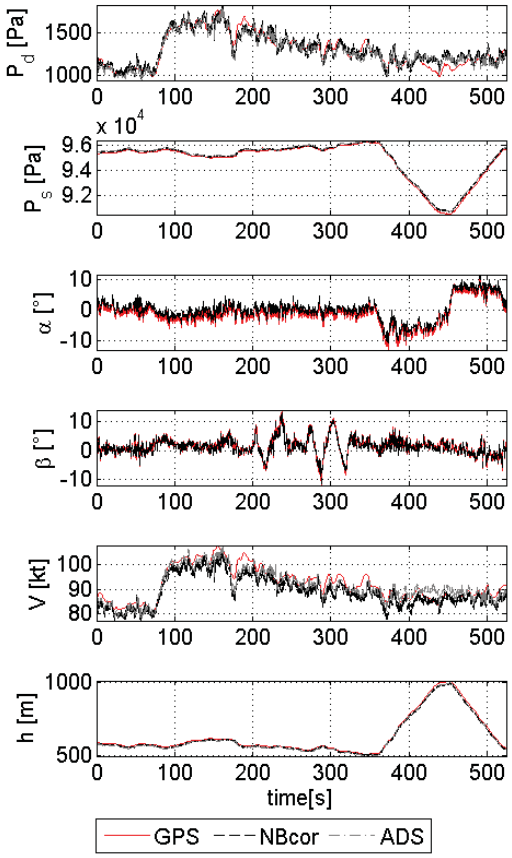

FIG.7. GPS/NB/ADS data 1st windbox, 80 kt to 100 kt

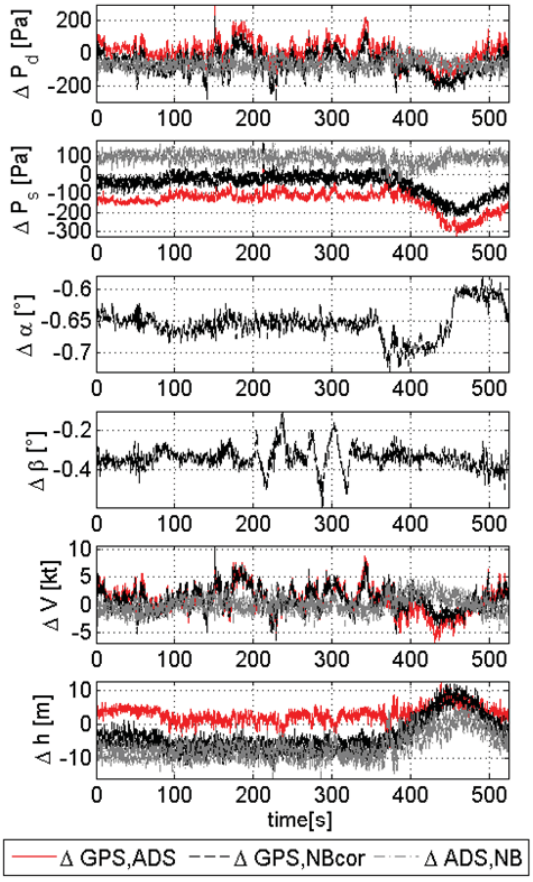

FIG.8. Difference GPS/NB/ADS data 1st windbox

their corresponding largest variation but the absolute difference to the reference data is always below 1° for both airflow angles. The difference in height is largest at the fifth and sixth leg with a difference of up to 10 m. This is not unduly large considering the accuracy of the GPS altitude information. The height information provided by the corrected noseboom static pressure is therefore deemed acceptable.

5.2. Coefficients Derived using Measured Wind

The wind measured during tower flyby tests by an anemometer mounted near the airport tower has to be subtracted from the measured ground speed of the helicopter. Via the thus calculated airspeed, the pressure calibration factors of the airspeed are determined: From the reference airspeed a reference dynamic pressure is calculated. The bias C_{P0} and the scale factor C_{P1} are determined to match the corrected dynamic noseboom pressure and the reference pressure in a least-square sense. Similar to the results obtained using the SCADS1 method, the dependency between C_{P0} and C_{P1} leads to large variances in these two parameters. The dependency is depicted in FIG.9.

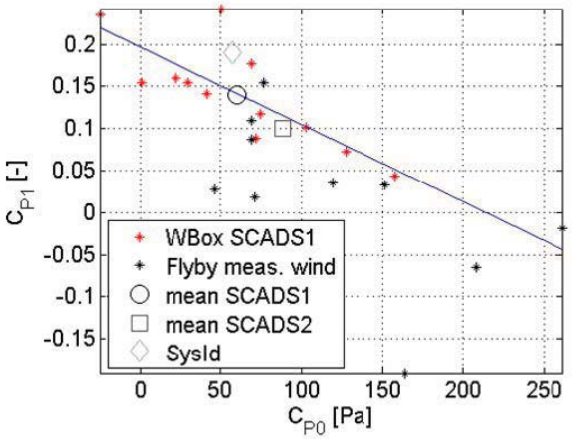

FIG.9. Pressure coefficient C_{P1} vs. $C_{P0,}$ SCADS windboxes and tower flybys

Although the data is even wider spread, the ratio between the coefficients is relatively similar to the one obtained for the windbox runs and the SCADS1 approach. Again, this large deviation in both correction factors is probably due to too little dynamic in one run alone. If both the bias factor C_{P0} and the scale factor C_{P1} are determined, the mean, maximum, minimum and standard deviation values of C_{P0} are 119.69 Pa, 261.26 Pa, 46.20 Pa and 68.75 Pa. The corresponding values of C_{P1} are .0145, .1543, -.1913 and .0930. Hence, to check the consistency with the correction factors derived via system identification, the multiplication factor is fixed to the system identification value of C_{P1} = 0.19. The resulting values are shown in TAB 6. If the scale factor is fixed to the system identification value of C_{P1} = 0.19, the mean of the bias is C_{P0} = 61.58 Pa, which corresponds well to the scale factor of the system identification from TAB 4, C_{P0} = 58.90 Pa. Due to this small difference, the difference in airspeed with the measured pressure corrected with these values is relatively small. The resulting speed variation at a measured dynamic pressure of 0 Pa is 0.42 kt. This error decreases further with increasing speed.

	C_{P0} [Pa] with C_{P1} = 0.19
Mean	61.58
Max	142.74
Min	21.99
Std. Dev.	44.05

TAB 6. Pressure correction coefficients obtained from pace car flybys

At a dynamic pressure of 1500 Pa the difference resulting from the difference in correction factors would be 0.06 kt, i.e. practically non existent. FIG.10 shows the application of the system identification correction parameters to data from a deceleration tower flyby. The reference airspeed is INS/GPS ground speed subtracted by measured wind. The airspeed derived with estimated wind is shown for comparison.

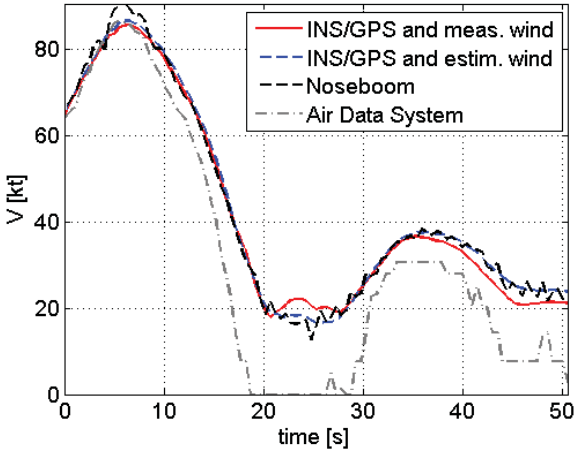

FIG.10. Airspeed comparison, deceleration tower flyby, 20 kt to 80 kt

The difference between measured and estimated airspeed is exemplarily shown for another tower flyby in FIG.11. Obviously, the deviations in the wind components cannot be modeled by constant wind. The difference between the measured and the estimated wind does not exceed 3 kt, though, and the difference to the mean of the measured data is below 0.5 kt for both components.

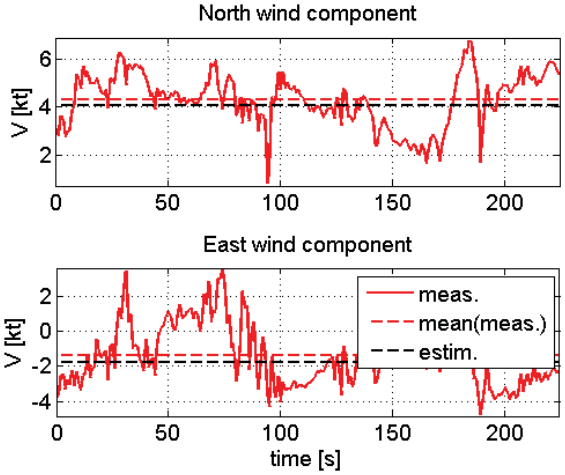

FIG.11.Comparison measured vs. estimated wind

At airspeed higher than 80 kt, the INS/GPS based airspeed and the ADS measurements agree well, as can be seen also in FIG.7 and FIG.8. The differences between air data system and reference airspeed increase considerably for airspeeds lower than 60°kt. For all airspeed below 60 kt, noseboom airspeed provides the only reliable, online-available airspeed data. It has to be determined down to which airspeed valid noseboom data can be obtained. For this purpose, the low speed pace car flight tests are undertaken

5.3. Correction Coefficients Pace Car Tower Flyby Measured Wind

To identify the lowest speed at which valid noseboom measurements are still measured, the pace car flybys were evaluated separately. The corresponding correction coefficients, derived with measured wind and with the bias C_{P1} = 0.19 fixed to the value obtained via system identification are listed in TAB 7. Only values for flights with speed at or above 30 km/h are used for the calculation of the mean and standard deviation. The values of the three lower speeds are not considered because the downwash clearly disturbs the dynamic pressure measurement at these speeds.

	C_{P0} [Pa] with C_{P1} = 0.19
5 km/h (2.7 kt)	35.925
10 km/h (5.4 kt)	39.05
20 km/h (10.8 kt)	70.01
30 km/h (16.2 kt)	59.49
40 km/h (21.6 kt)	65.44
50 km/h (27.1 kt)	71.165
Mean (30-50 km/h)	65.36
Std. dev. (30-50 km/h)	5.83

TAB 7. Pressure correction coefficients obtained from pace car flybys

In FIG.12 and FIG.13, the reference dynamic pressure as derived from INS/GPS and measured wind is compared to corrected noseboom and air data system data. The figures illustrate the difference between disturbed noseboom measurements, FIG.12, and valid noseboom measurements, FIG.13. FIG.12 shows the resulting dynamic pressures and velocities for the third pace car run at 20 km/h and FIG.13 for the fourth run at 30 km/h. The noseboom measurements are corrected with the mean SCADS1 coefficients from TAB 1.

When the air data measurement system, mounted below the helicopter, is corrupted by rotor downwash, the dynamic pressure measurements become negative. For this case, a velocity of zero is indicated by the air data system. The corrected noseboom dynamic pressure is close to zero, but not negative. Still, s the downwash influences the noseboom measurement, too, these measurements at airspeed of 10.8 kt are very noisy. At 16.2 kt, depicted in FIG.13, it can be seen that the airspeed of the corrected noseboom is a good match to the reference airspeed. At this airspeed, the pitot tube of the basic air data system is still influenced by rotor downwash and yields negative i.e. invalid dynamic pressure and no airspeed. The offset for the fourth, fifth and sixth run at 16.2 kt, 21.6 kt and 27.1 kt are close to the offset C_{P0} = 58.90 Pa as derived via system identification and close to the mean of the values calculated by the SCADS1 method, C_{P0} = 60.20 Pa. Hence, measured dynamic pressure corrected with those values gives a good fit of reference to noseboom speed.

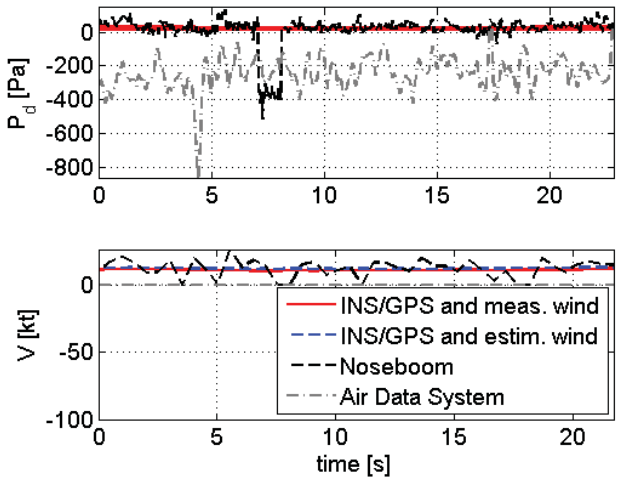

FIG.12. Dynamic pressure and airspeed, pace car, 10.3 kt

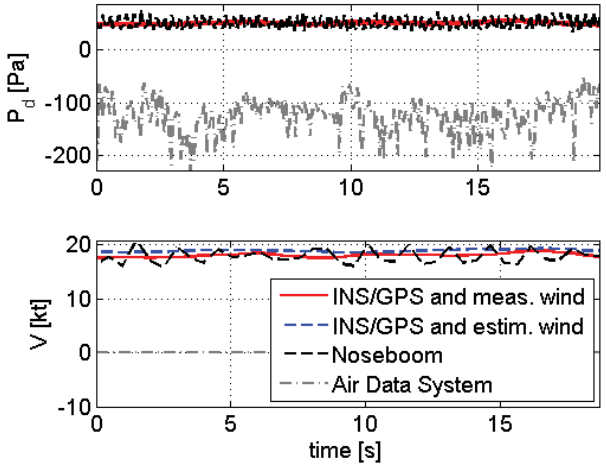

FIG.13. Dynamic pressure and airspeed, pace car, 16.2 kt

6. CONCLUSION

The SCADS (Simultaneous Calibration of Air Data Systems) technique has been used to dynamically calibrate the noseboom measurements of the EC-135 FHS of DLR. Due to the availability of a high-precision INS/GPS system with an integrated Kalman filter, no separate filtering is necessary to generate trajectory reference data. Both the pressure measurements from the pitot system and the airflow angle values from the airflow vanes are calibrated and the results compared with those from classical approaches such as tower flybys and flight path reconstruction techniques.

The results show

- corrected noseboom measurements are valid for velocities down to 16.2 kt.
- airspeeds calculated from corrected noseboom measurements agree well with reference data from INS/GPS ground speed measurements subtracted by wind, see FIG.7 and FIG.8

– airspeeds calculated from corrected noseboom measurements agree well with airspeed from an air data system mounted below the helicopter for airspeeds from 40 kt to 110 kt
– variations in calculated airspeed due to differences in correction factors remained acceptable for velocities from 16.2 kt to 110 kt, although the correction factors are derived with different data sets, different optimization methods and different cost functions
– airspeed, calculated based on correction factors obtained with estimated wind, compares well with airspeed derived with measured wind data
– angle of attack correction leads to mean differences to reference data smaller than 1° for airspeeds higher than 30 kt
– sideslip angle correction leads to mean differences to reference data smaller than 1° for airspeeds higher than 16.2 kt

The calculated signals, derived with the identified correction terms, provide the desired accuracy and widen the range in which airspeed can be detected via dynamic pressure measurement considerably in comparison with the standard air data system. The resulting airspeed and airflow angle information are to be used to provide accurate speed information over a wider speed range which is needed in current projects e.g. for stabilization and trajectory control and system identification purposes.

7. REFERENCES

[1] K. Hui, S. Baillie: *Validation of the Simultaneous Calibration of Aircraft Position Error and Airflow Angles Using a Differential GPS Technique on a Helicopter*, 1996

[2] K. Hui: *Application of the Simultaneous Calibration of Aircraft Position Error and Airflow Angles Using a Differential GPS Technique on a Bell 212 Helicopter*, Institute for Aerospace Research, Flight Research Laboratory, Laboratory Memorandum, 1998

[3] B. Leach, K. Hui: *In-flight Technique for Calibrating Air Data Systems Using Kalman Filtering and Smoothing*, AIAA Atmospheric Flight Mechanics, Montreal, 2001

[4] V. Parameswaran, R. Jategonkar, M. Press: *Five-Hole Flow Angle Probe Calibration from Dynamic and Tower Flyby Maneuvers*, Journal of Aircraft, Vol. 42, No.1, January-February, 2005

[5] S. Seher-Weiß: *Kompatibilitätskontrolle und Nasenmastkalibrierung*, Institutsbericht IB 11-2009/31

[6] N.N.: *Technical Data for Universal Nose Data Boom SAC P/N 100510 and Accessory*, SpaceAge Control Inc., 1997

[7] N.N.: *Prime Item Development Specification for the H-764GU GATM Upgrade Embedded GPS/INS*, Specification No. DS 34209200 Rev F, 2002

[8] N.N.: *Windrichtungsgeber*, Thies Clima, Bedienungs-anleitung 020889/11/07

[9] N.N.: *SHARPE XR6 (including RPS), GPS Receiver, User Manual,* Symmetricom Ltd.

[10] P. Guichard: *ADS3000 SYSTEM REQUIREMENT DOCUMENT DLR03*, 1997

[11] H. Schlichting, E. Truckenbrodt: *Aerodynamik des Flugzeuges*, Erster Band, Springer-Verlag Berlin/ Heidelberg/New York, 1967

[12] R.V. Jategaonkar: Flight Vehicle System Identification: *A Time Domain Methodology, AIAA Progress in Astronautics and Aeronautics*, Vol. 216, 2006, ISBN 1-56347-836-6